Reconfigurable Terahertz Metamaterials

Hu Tao,[1] A. C. Strikwerda,[2] K. Fan,[1] W. J. Padilla,[3] X. Zhang,[1,*] and R. D. Averitt[2,†]

[1]*Department of Mechanical Engineering, Boston University, 110 Cummington Street, Boston, Massachusetts 02215, USA*
[2]*Department of Physics, Boston University, 590 Commonwealth Avenue, Boston, Massachusetts 02215, USA*
[3]*Department of Physics, Boston College, 140 Commonwealth Avenue, Chestnut Hill, Massachusetts 02467, USA*

(Received 29 July 2009; revised manuscript received 10 September 2009; published 2 October 2009)

We demonstrate reconfigurable anisotropic metamaterials at terahertz frequencies where artificial ''atoms'' reorient within unit cells in response to an external stimulus. This is accomplished by fabricating planar arrays of split ring resonators on bimaterial cantilevers designed to bend out of plane in response to a thermal stimulus. We observe a marked tunability of the electric and magnetic response as the split ring resonators reorient within their unit cells. Our results demonstrate that adaptive metamaterials offer significant potential to realize novel electromagnetic functionality ranging from thermal detection to reconfigurable cloaks or absorbers.

DOI: 10.1103/PhysRevLett.103.147401 PACS numbers: 78.20.Ci, 77.22.Ch, 78.47.−p

The interaction of electromagnetic radiation with matter provides the means to control its amplitude, direction, polarization, wavelength, and phase. Quite generally, this necessitates a reduction from the symmetry of free space. At an interface between two otherwise isotropic substances, broken spatial inversion symmetry enables refraction as embodied by Snell's law. For propagation within a crystalline environment, it is anisotropic materials which provide the greatest ability to manipulate radiation. For example, uniaxial materials allow for polarization control and crystals which break inversion symmetry enable generation of even harmonics of the incident radiation. Metamaterials (MM) are artificial composites where the anisotropy and associated electromagnetic (EM) functionality are specified through the design and orientation of subwavelength particles within well-defined unit cells.

The response to electromagnetic (EM) radiation is encoded in constitutive relations explicitly appearing in Maxwell's equations. For anisotropic atomic-based materials, this requires a tensorial description of the electric permittivity ϵ_{ij} and magnetic permeability μ_{ij} the form of which is determined by symmetry. Metamaterials must obey the same constraints imposed by the symmetry of the local environment [1,2]. This poses both challenges and opportunities. For example, the realization of an isotropic MM exhibiting a negative refractive index remains unrealized while, in contrast, the function of an EM cloak requires specifically tailored ϵ_{ij} and μ_{ij} which are anisotropic (and, further, nonuniform) [3]. Of course, metamaterials have many other uses to control and manipulate EM radiation including the polarization, directionality, and amplitude, with many recent examples presented along these lines [3–10]. To control the anisotropy is to control the EM properties.

It is this ability to create and specify EM properties—from the microwave to the visible—that imbue MM with such potential. An additional aspect that has recently received considerable attention is the active control of the EM response to create functional devices such as modulators, tunable filters, etc. This has primarily been accomplished through optical or voltage control of the capacitive response of SRRs [11–13]. Another approach is to create MM where the anisotropic elements reorient within the unit cells in response to an external stimulus such as applied current or a change in the ambient temperature. This would be similar to a reorientational transition as occurs in many atomic-based materials.

To understand how this can be accomplished using metamaterials, it is important to consider the anisotropic response of the split ring resonator (SRR) [14,15]. Figure 1(a) depicts a SRR along with two cantilever legs whose function will be described shortly. In the quasistatic limit for incident EM radiation at the resonant frequency of

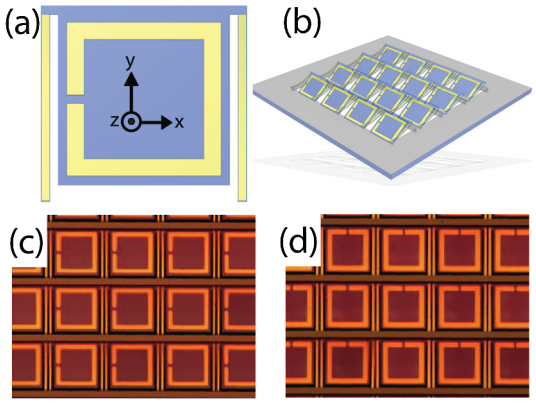

FIG. 1 (color online). (a) Unit cell consisting of a split ring resonator and cantilever legs. (b) Schematic view of a portion of the metamaterial structure highlighting how the SRRs rotate as the cantilever legs bend. (c) and (d) Photographs of portions of two of the THz metamaterial arrays fabricated for this study. The SRRs are 72 μm × 72 μm with an in-plane periodicity of 100 μm and an overall dimension of 1 cm × 1 cm.

the SRR, a component of the magnetic field parallel to the z axis (H_z) will drive the magnetic dipole (m_{zz}) of the SRR while a component of the electric field along the y axis (E_y) will drive the electric dipole (p_{yy}) response. These responses lead to terms μ_{zz} and ϵ_{yy} terms in the anisotropic permeability and permittivity, respectively [1]. In addition, SRRs are bianisotropic, meaning that E_y contributes to m_{zz} and H_z contributes to p_{yy}. The bianisotropic response leads to complexity in characterizing the full EM response while offering the means to create novel functional responses. The extent to which m_{zz} or p_{yy} is driven depends sensitively on projection of the components of H along z and, similarly, E along y. The electromagnetic response is thus a sensitive function of orientation.

Tuning of the EM response requires the means to control the orientation of the SRRs within the unit cells. The two cantilever legs on either side of the SRR in Fig. 1(a) serve such a purpose. This is more easily visualized in Fig. 1(b) where each SRR in a periodic array is attached to a supporting substrate via the cantilevers. If the cantilever bends in response to an external stimulus, the SRRs will bend out of the plane of the substrate which will lead to dramatic changes in the electromagnetic response. Figures 1(c) and 1(d) show photographs of portions of the cantilever SRR structures we have fabricated. The orientation of the SRRs [e.g., the 90° rotation of the SRR from Fig. 1(c) to 1(d)] with respect to the cantilevers will also affect the EM response.

The metamaterial structures shown in Figs. 1(c) and 1(d) were fabricated using surface micromachining technology. The process consists of four steps: deposition of silicon nitride (SiN_x) films, patterning of the Au (200 nm thick) layer for the SRRs and cantilever legs, patterning the SiN_x film for supporting plate and bending legs, and release of the structure by KOH etching. This results in an array of free-standing SRRs which are connected to the supporting substrate by the cantilever legs. The periodicity of the array is 100 μm, with the overall dimensions of the SRR 72 μm $\times$ 72 μm and the overall dimensions of the array are 1 cm $\times$ 1 cm. The difference in the thermal expansion coefficients of SiN_x and Au is such that a change in temperature leads to a bending of the cantilever supports. By changing the temperature, SRRs which initially lie in the plane of the substrate will bend up out of plane. For ease of fabrication and characterization, we have chosen a thermal tuning approach. However, other MEMS-based approaches such as electrostatic or piezoelectric actuation would enable similar reconfigurability albeit with a slight increase in complexity.

To characterize the electromagnetic response as a function of orientation, terahertz time-domain spectroscopy (THz-TDS) was employed [16,17]. The THz electric field was coherently measured after transmission through the metamaterial sample and a suitable reference, which in this case is air (i.e., the sample is simply removed). Fourier transformation of the time-domain waveforms then provided the frequency dependent THz electric field amplitude and phase. Dividing the sample spectrum by the reference we obtain the normalized field transmission $T(\omega)$ and phase $\Phi(\omega)$ of the metamaterial sample. All measurements were performed at normal incidence. To characterize changes in transmission associated with reorientation of the SRRs within the unit cells, a procedure was employed to lock in the orientation. Rapid thermal annealing (RTA) at a specific temperature sets the orientation of the SRRs at a particular angle with respect to the substrate. Following each THz-TDS measurement, RTA at a higher temperature would lead to a further increase in the bending. In this way, it was possible to measure response over a large angular range from 0 to nearly 90° (i.e., the SRRs in-plane the plane of the substrate to nearly perpendicular). In particular, RTA from 350 to 550 °C was performed in steps of 50 °C. To better understand the measured response, CST MICROWAVE STUDIO was used to simulate the electromagnetic response as a function of the orientation as described below.

Figure 2 displays the experimental results. In Fig. 2(a), SEM pictures show a portion of the MM arrays at various out-of-plane angles. At each orientation the terahertz trans-

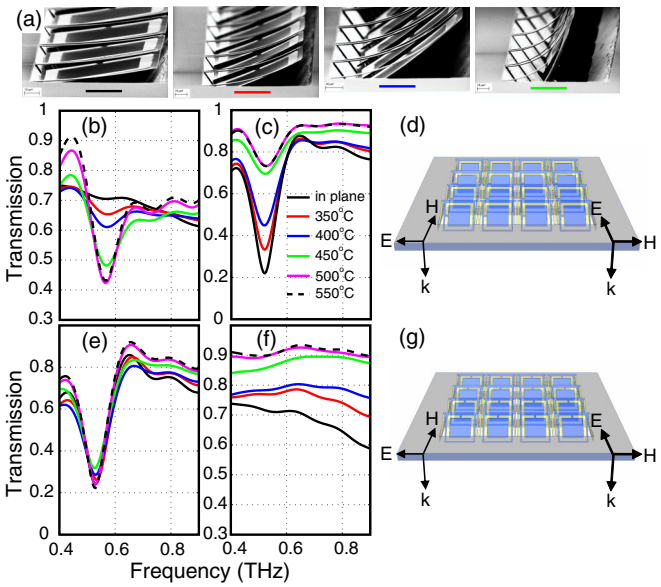

FIG. 2 (color online). (a) SEM pictures showing the bending of the SRRs following KOH release (first picture) and RTA at 350, 400, and 450 °C. (b) Magnetic Response: Transmission as a function of frequency for various orientations of the SRRs. The black curve is with the SRRs lying in the plane of the substrate, red curve—RTA 350 °C, blue curve—RTA 400 °C, green curve—RTA 450 °C, magenta curve—RTA 500 °C, dashed black curve—RTA 550 °C. (c) Electric Response: color code is same as for (b). (d) Schematic showing the polarization for (b) (on left) and (c) (on right). (e) Bianisotropic response: color code as for (b) and (c). (f) Nonresonant response. (g) Schematic showing the polarization for (e) (on left) and (g) (on right).

mission was measured for two polarizations. First, we consider the results of Fig. 2(b) and 2(c). Figure 2(d) depicts the orientation [see also Fig. 1(c)] of the metamaterial-cantilever arrays with the polarization of the incident radiation corresponding to the results of Fig. 2(b) shown on the left and the polarization for Fig. 2(c) shown on the right. For Fig. 2(b), when the SRRs lie in plane, the incident polarization is such that neither E or H drives the magnetic or electric response of the SRRs. Thus, the transmission (black line) as a function of frequency is featureless. However, as the cantilever legs bend upward, the SRRs gradually bend out of plane. As this occurs, a component of H drives the magnetic dipole resulting in the appearance of a weak resonant feature at ~500 GHz (red line). With increasing bending of the cantilever legs and commensurate reorientation of the SRRs, the magnetic resonance strength increases which, in turn, leads to a strong decrease in transmission. Eventually, the resonant response is maximized as the cantilever bending angle saturates at an angle of approximately 65°. As no component of E projects along the y direction for any orientation of the SRRs (one can consider the Cartesian coordinates depicted in Fig. 1(a) as rotating with the SRRs as they reorient while E and H remain fixed), the bianisotropy does not affect the transmission. Thus, the 30% decrease in transmission results from a magnetic resonance that is driven entirely by the incident magnetic field. The magnetic response of the MM is determined and controlled by the orientation of the SRRs within the unit cells.

In Fig. 2(c), the polarization is rotated by 90° in comparison to Fig. 2(b). For this case, with the SRRs in plane, the electric field E drives circulating currents leading to a strong decrease in the transmission at 500 GHz (black line). Now, however, as cantilever bending reorients the SRRs out of the plane of the substrate, the projection of E along y decreases leading to a gradual decrease in the resonance strength. For any orientation of the SRRs, no component of H ever pierces the plane of the SRR and thus no magnetic resonance or bianisotropic response is possible. The resonant response is purely electric.

The measurements were repeated with the SRRs rotated by 90° with respect to the cantilever legs [as in Fig. 1(d)]. The result are shown in Fig. 2(e) to 2(g), with Fig. 2(g) depicting the geometry and with the polarization on the left (right) corresponding to the data in Fig. 2(e) [Fig. 2(f)]. For Fig. 2(e), for any angle of the SRR with respect to the plane of the substrate, the electric resonance will be driven. Upon increasing the out-of-plane angle, the magnetic resonance will also be driven as H couples to the magnetic dipole along z. Nevertheless, as the data reveal, there is no substantial change in the resonance transmission. This constant transmission as a function of angle results from the bianisotropy of the SRRs which now plays an important role [in contrast to Figs. 2(b) and 2(c)]. In particular, no change in the resonant response is expected as a function of orientation if, approximately, the magnetic polarizability times the electric polarizability is equal to minus the square of the magnetoelectric polarizability [1]. Such an equality holds for SRRs whereby, as a function of orientation, any decrease in the total electric dipole response (driven by E and H) is compensated by an increase in the total magnetic dipole response as described in the supplementary information available online [18].

Finally, for the polarization corresponding to the data in Fig. 2(f), the incident EM radiation does not couple to the resonant electric or magnetic dipolar response for any angle of the SRRs as they bend out of plane. However, as the SRRs reorient out of the plane of the substrate there is a broadband increase in the transmission. This response results from the fact that there are higher frequency electric dipole resonances associated with the cantilever legs and in-phase currents driven in the SRRs [19]. As the cantilever legs and SRRs reorient out of the plane defined by the substrate, the E field component projected along the dipoles decreases leading to an increased transmission that approaches 90% (see also [18]).

As these results reveal, the reorientation of the SRRs leads to dramatic changes in the electromagnetic response. In principle, the EM response in Fig. 2(b) [Fig. 2(c)] can be understood in terms of an effective medium description of the electric permittivity ϵ_{yy} (magnetic permeability μ_{zz}). The bianisotropic response which was discussed in regards to Fig. 2(e) is described in terms of a separate magnetoelectric susceptibility and does not appear explicitly in either μ_{zz} or ϵ_{yy}. The configuration of the MM in Fig. 2(e) with strong bianisotropy is ostensibly the most complex to describe in terms of the constitutive relations, yet yields the simplest electromagnetic response.

To better understand the EM response for the various orientations of the SRRs in Fig. 2, simulations of the cantilever-MM structure were performed using CST MICROWAVE STUDIO. The structure was modeled as depicted in Fig. 1(a), where the two bimaterial cantilevers are taken to be a constant length, and then curved at a constant bending angle to achieve the desired angle of deflection for the planar MM structure suspended between them. Figure 3(a) shows the results of simulations of the transmission as a function of frequency for the reconfigurable magnetic response in Fig. 2(a). The simulations, from in-plane at 0° to 80°, largely agree with the experimental results. Namely, as the SRRs bend out of the plane of the substrate, activation of the magnetic resonance results in a decrease in the transmission. Figure 3(b) shows the complex magnetic permeability $\mu_{zz} = \mu_{\text{real}} + i\mu_{\text{imag}}$ extracted from the full-wave simulations for the structure at 90° assuming a cubic unit cell [20]. A reasonable Lorentzian-like response is obtained highlighting the magnetic nature of the resonance. The experimental resonance is somewhat weaker and broader in comparison to the

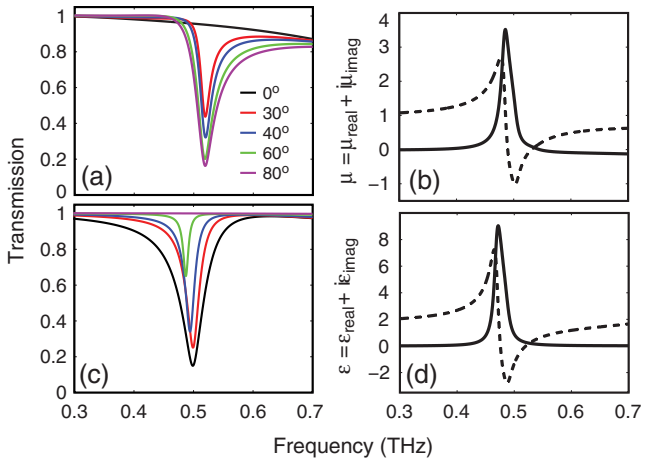

FIG. 3 (color online). (a) Magnetic response: Transmission as a function of frequency for various bending angles (0°—SRR in the plane of the substrate, 90°—perpendicular to the plane of the substrate). Black—0°, red—30°, blue—40°, green—60°, magenta—80°. (b) The extracted permeability with the SRRs at 90°. Black line is the imaginary part of μ_{zz} and the dashed line is the real part. (c) Electric Response: Transmission as a function of frequency for various bending angles. Color code is same as for (a). (d) The extracted electric permittivity with the SRRs at 0°. Black line is the imaginary part of ϵ_{yy} and the dashed line is the real part.

simulation results. This likely arises from effective inhomogeneous broadening due to fabrication tolerances and slight variability in the cantilever leg bending angles across the 1 cm^2 structure. Figure 3(c) shows simulations corresponding to the reconfigurable electric response of Fig. 2(c). There is also reasonable agreement between the data and the simulations. For 80° (magenta line) the resonance has vanished. For the largest experimental bending a resonance is still present clearly indicating that such a 80° bending angle has not been experimentally achieved. This is also consistent with the SEM measurements. Figure 3(d) shows that with the SRRs lying in-plane (0°) a reasonable Lorentzian-like response for the $\epsilon_{yy} = \epsilon_{\text{real}} + i\epsilon_{\text{imag}}$ is obtained. We note that simulations of the response corresponding to the configurations in Figs. 2(e) and 2(f) are also in agreement with experiment as described in Ref. [18].

Our experimental and simulation results reveal that it is possible to create reconfigurable metamaterials where reorientation of the SRRs leads to a tunable electromagnetic response that is dominantly electric or magnetic in nature. For these initial proof-of-principle measurements, RTA was used to lock the SRRs into a set orientation. This facilitated electromagnetic characterization using THz-TDS. However, in actual operation, it will be possible to actively reorient the SRRs using well-developed actuation techniques which include resistive, piezoelectric, and electrostatic actuation [21–23]. Potential applications include reconfigurable filters, negative index surfaces, thermal cantilever-based detection, or fine tuning of the electric or magnetic response for optimizing perfect absorbers or transformation optics derived metamaterials such as cloaks or concentrators. Furthermore, in the present demonstration of reconfigurable MMs, each of the SRRs was designed to reorient in an identical fashion in response to an external stimulus. More complex materials could be designed where a fraction of the unit cells remain stationary or different unit cells move in orthogonal directions.

We acknowledge partial support from the Los Alamos National Laboratory LDRD program, DOD/Army Research Laboratory under Contract No. W911NF-06-2-0040, NSF under Contract No. ECCS 0802036, and DARPA under Contract No. HR0011-08-1-0044. The authors would also like to thank the Photonics Center at Boston University.

*xinz@bu.edu
†raveritt@physics.bu.edu

[1] R. Marques, F. Medina, and R. Rafii-El-Idrissi, Phys. Rev. B **65**, 144440 (2002).
[2] W. J. Padilla, Opt. Express **15**, 1639 (2007).
[3] D. Schurig *et al.*, Science **314**, 977 (2006).
[4] N. Fang, H. Lee, C. Sun, and X. Zhang, Science **308**, 534 (2005).
[5] T. J. Yen *et al.*, Science **303**, 1494 (2004).
[6] N. I. Landy *et al.*, Phys. Rev. Lett. **100**, 207402 (2008).
[7] A. C. Strikwerda *et al.*, Opt. Express **17**, 136 (2009).
[8] S. Linden *et al.*, Science **306**, 1351 (2004).
[9] S. Zhang *et al.*, Phys. Rev. Lett. **95**, 137404 (2005).
[10] A. Alù and N. Engheta, J. Opt. A **10**, 093002 (2008).
[11] W. J. Padilla *et al.*, Phys. Rev. Lett. **96**, 107401 (2006).
[12] H. T. Chen *et al.*, Nature (London) **444**, 597 (2006).
[13] H. T. Chen *et al.*, Nat. Photon. **2**, 295 (2008).
[14] J. B. Pendry *et al.*, IEEE Trans. Microwave Theory Tech. **47**, 2075 (1999).
[15] D. R. Smith, W. J. Padilla, D. C. Vier, S. C. Nemat-Nasser, and S. Schultz, Phys. Rev. Lett. **84**, 4184 (2000).
[16] D. Grischkowsky *et al.*, J. Opt. Soc. Am. B **7**, 2006 (1990).
[17] M. Tonouchi, Nat. Photon. **1**, 97 (2007).
[18] See EPAPS Document No. E-PRLTAO-103-025942. Further information on the fabrication, electromagnetic simulations, bianisotropic response, higher frequency dipolar response, and line broadening can be found on EPAPS (es2009jul29_079). For more information on EPAPS, see http://www.aip.org/pubservs/epaps.html.
[19] W. J. Padilla *et al.*, Phys. Rev. B **75**, 041102(R) (2007).
[20] D. R. Smith *et al.*, Phys. Rev. E **71**, 036617 (2005).
[21] L. Wu and H. Xie, IEEE J. Sel. Top. Quantum Electron. **13**, 316 (2007).
[22] Y. Yee *et al.*, Sens. Actuators A, Phys. **89**, 166 (2001).
[23] C. Pu *et al.*, IEEE J. Sel. Top. Quantum Electron. **10**, 472 (2004).